General Disclaimer

One or more of the Following Statements may affect this Document

- This document has been reproduced from the best copy furnished by the organizational source. It is being released in the interest of making available as much information as possible.

- This document may contain data, which exceeds the sheet parameters. It was furnished in this condition by the organizational source and is the best copy available.

- This document may contain tone-on-tone or color graphs, charts and/or pictures, which have been reproduced in black and white.

- This document is paginated as submitted by the original source.

- Portions of this document are not fully legible due to the historical nature of some of the material. However, it is the best reproduction available from the original submission.

Produced by the NASA Center for Aerospace Information (CASI)

NATIONAL AERONAUTICS AND SPACE ADMINISTRATION

Technical Memorandum 33-573

The Mariner Mars 1971 Radio Frequency Subsystem

R. S. Hughes

(NASA-CR-130866) THE MARINER MARS 1971 RADIO FREQUENCY SUBSYSTEM (Jet Propulsion Lab.) 51 p HC $4.75 CSCL 17B

N73-17164

Unclas

G3/07 63444

JET PROPULSION LABORATORY
CALIFORNIA INSTITUTE OF TECHNOLOGY
PASADENA, CALIFORNIA

December 1, 1972

NATIONAL AERONAUTICS AND SPACE ADMINISTRATION

Technical Memorandum 33-573

The Mariner Mars 1971 Radio Frequency Subsystem

R. S. Hughes

JET PROPULSION LABORATORY
CALIFORNIA INSTITUTE OF TECHNOLOGY
PASADENA, CALIFORNIA

December 1, 1972

Prepared Under Contract No. NAS 7-100
National Aeronautics and Space Administration

PREFACE

The work described in this report was performed by the Telecommunications Division of the Jet Propulsion Laboratory.

CONTENTS

I. Introduction 1

II. Design Changes 2

III. Procurement Process and Hardware Delivered 3

IV. Telemetry Channels 4

V. RFS Commands 8

VI. RFS Subassemblies 8

A. Receiver and Diplexer Subassembly 8

B. Exciter Subassembly 10

C. Control Unit 15

D. Traveling Wave Tube Amplifiers 16

E. Microwave Components 18

VII. RFS Performance and Test History 23

A. Contractor Tests 23

B. JPL Receiving Tests 23

C. Spacecraft/RFS Integration Tests 24

D. Subsystem Tests 24

E. Spacecraft/RFS Mission Compatibility Tests 24

F. Electromagnetic Interference Tests 25

G. DSIF Compatibility Tests 25

H. Miscellaneous Tests 26

I. Recommendations for Improvements in Testing 26

J. AFETR Tests 28

K. Miscellaneous Problems and Recommendations 30

PRECEDING PAGE BLANK NOT FILMED

CONTENTS (contd)

TABLES

1. Design values of significant RFS parameters 32

2. Radio modes 33

3. Design changes 34

4. RFS commands 36

5. Electrical comparison of MM'69 ×24 and MM'71 ×30 multipliers 37

6. Typical TWTA major performance parameters 38

7. Microwave component electrical characteristics 39

FIGURES

1. MM'71 RFS 40

2. Radio frequency subsystem block diagram 41

3. Receiver block diagram 42

4. Exciter block diagram 43

5. ×30 block diagram 43

6. Control unit block diagram 44

7. TWTA block diagram 44

ABSTRACT

This report describes the radio frequency subsystem (RFS) for the Mariner Mars 1971 (MM'71) spacecraft. The MM'69 RFS was used as the baseline design for the MM'71 RFS, and the report describes the design changes made to the 1969 RFS for use on MM'71. It also cites various problems encountered during the fabrication and testing of the RFS, as well as the types of tests to which the RFS was subjected. In areas where significant problems were encountered, a detailed description of the problem and its solution is presented. In addition, the report contains some recommendations for modifications to the RFS and test techniques for future programs.

I. INTRODUCTION

The Mariner Mars 1971 (MM'71) radio frequency subsystem (RFS) provides the communication link between the spacecraft and the ground-based Deep Space Instrumentation Facility (DSIF). The functions of the RFS, shown in Fig. 1, are to

(1) Receive the S-band radio frequency signal transmitted from the DSIF.

(2) Demodulate the S-band signal and provide the extracted composite command signal to the flight command subsystem.

(3) Demodulate the ranging signal transmitted from the DSIF.

(4) Transmit a modulated RF signal with a carrier which is phase-coherent with either the received carrier or with an internally generated frequency source.

(5) Modulate the transmitted carrier with the composite telemetry signal from the flight telemetry subsystem.

(6) Modulate the transmitted carrier with the receiver-detected ranging signal.

The RFS consists of the four subassemblies and the microwave components shown in Fig. 2. The major subassemblies are the receiver, the exciter, the traveling wave tube amplifier (TWTA), and the control unit subassemblies. The microwave components consist of the dual RF switch, the filter hybrid, the output filter, and the diplexer.

The design performance parameters and the operational modes of the RFS are shown in Tables 1 and 2, respectively.

II. DESIGN CHANGES

The Mariner Mars 1969 (MM'69) RFS served as a design baseline for the MM'71 RFS, and several changes were required to implement modifications in system configuration and operational characteristics. In addition, changes were made to increase reliability. The significant changes incorporated into the MM'71 RFS were:

(1) The self-lock/false-lock problems which occurred in MM'69 were eliminated by modifying several receiver modules and changing the ×5-×24 frequency multiplier in the exciter chain to a ×4-×30 combination. However, the design of the ×30 multiplier in the exciter was changed late in the program to incorporate a breakdown suppressant when it was determined that the ×30 RF breakdown margin was inadequate.

(2) An active loop filter was implemented into the receiver which increased the loop gain by 10.

(3) The capability of turning the TWTA off and on was added. As part of this change, heaters were added to the RFS bay.

(4) A dual trace concept was incorporated into those microwave components employing stripline techniques. However, when a RF breakdown occurred in the proof-test model (PTM) and Flight 1 circulator switch, the dual trace was removed from the switch and other design changes were made to improve its breakdown margin.

(5) The control unit was modified to incorporate the new antenna switching logic and the central computer and sequencer (CC&S) 2B transmit on the low-gain antenna (LGA) event.

(6) The voltage-controlled oscillator/auxiliary oscillator (VCO/AUX OSC) transfer inhibit was included as an umbilical function.

These changes required modifications in several modules. Also, as stated, design deficiencies were encountered late in the program both by the RFS subsystem contractor and at JPL which required additional design

changes. The significant design changes or modifications finally incorporated into the RFS are listed in Table 3 and discussed in more detail in Section VI.

There are four distinct RFSs: prototype, PTM, Flight 1, and Flight 2, as defined in the next section. The prototype radio was used to define the system design, and design documentation for the PTM and flight systems was based upon prototype performance. The design and test specifications were updated and revised after prototype tests were completed. Although the prototype performance was generally adequate, it was necessary to make design changes in some of the PTM modules.

III. PROCUREMENT PROCESS AND HARDWARE DELIVERED

The procurement process for MM'71 was somewhat different from that of MM'69. In MM'69 the complete flight RFS was purchased from a single contractor. However, in MM'71 the microwave components, the traveling wave tube (TWT), and TWTA were purchased separately by JPL from three different contractors and then supplied to the RF subsystem contractor. The subsystem contractor integrated the JPL-supplied hardware along with his own into the RFS and conducted the flight-qualification testing. The contracts for the microwave components, TWT, and TWTA were fixed-price. The RFS was purchased on a cost-plus-fixed-fee contract. Under these contracts, the four complete RFS assemblies listed below were delivered.

(1) Prototype--a non-flight, reworked and modified MM'69 prototype RFS.

(2) PTM (S/N 001)--the type-approval and flight spare unit, which was the reworked and modified MM'69 PTM.

(3) Flight 1 S/N 003--the MM'69 flight spare, reworked and modified for MM'71, which was used on Mariner 8.

(4) Flight 2 S/N 005--a new assembly, used on Mariner 9.

IV. TELEMETRY CHANNELS

A number of RFS parameters are telemetered during flight. Each analog quantity is quantized to 7 bits, providing 128 distinct values (0-127 DN*). These measurements are necessary to provide engineering data for equipment performance evaluation and analysis. The channels, which indicate uplink signal strength, antenna RF drive level, VCO frequency, and temperature, are operational functions that aid in tracking the spacecraft and provide information for telecommunications predictions. Other channels, such as exciter voltage, exciter drive, TWT anode voltage, TWT helix current, and local oscillator drive are used to assess the performance of the various subsystems. In general, the channels were mechanized so that the 0-127 DN range covers a minimum of 80% of the available voltage telemetry range. While the telemetry channels as mechanized on MM'71 are generally satisfactory, some changes, such as calibration, could be made to improve the accuracy and usefulness of some channels on future projects. The channels are discussed below, and recommendations for changes and improvements are made for each of them.

(1) Receiver static phase error, channel 111 (±63 kHz at S-band, converted to ±1.5 V). Channel 111 is a measure of the VCO control voltage and indicates the receiver VCO operating frequency. The ±63-kHz range occupies about 85 to 90% of the available range of 0-127 DN.

(2) Automatic gain control, channel 115 (0-3V). Channel 115 indicates the spacecraft received signal level and whether the receiver is in or out of lock. As now mechanized, the channel provides signal level data from -70 dBm to threshold (-153 dBm) and typically uses about 2-1/2 V of the available 3-V range. Signal levels above -100 dBm are not experienced in flight. Finer resolution could be obtained if the range were reduced to -100 dBm to threshold. Improvement of the calibration of this channel over the temperature range prevailing in flight would also permit more accurate signal level measurement.

---

*DN = Data Number.

(3) Exciter drive, channel 210 (0-100 mW, converted to 0-100 mV). Channel 210 measures the RF output power of the exciter and thus the drive to the TWTA. The typical maximum resolution of channel 210 per data number is 0.03 dB, and the minimum is 0.06 dB. The channel also drifts one data number for each 0.5 to 1.1°C of temperature change. The calibration of the channel, as well as that of 213 and 214 described below, was inadequate for the following reasons:

(a) The channel was calibrated only at room temperature and the flight acceptance FA limits. Additional calibration should have been done at the expected flight temperature limits, which are typically 10 to 34°C.

(b) Only the test chamber temperature was noted at the time of calibration. If the calibration is to be useful, it must, as a minimum, include the VCO telemetered temperature channel 404 (described below). An additional improvement in calibration could be obtained by installing flight temperature transducers next to the diode detector. An alternate action would be to improve the temperature stability of this channel.

(4) RF drive monitor, high-gain antenna (HGA), channel 213 (0-25 W, converted to 0-100 mV). Channel 213 monitors the RF drive from the TWTA to the high-gain antenna. The approximate resolution is 0.1 dB per data number. This channel has the same problem of drift with temperature as channel 210, and it also lacked a good temperature calibration in MM'71.

(5) RF drive monitor, LGA, channel 214 (0-25 W, converted to 0-100 mV). Channel 214 monitors the RF drive from the TWTA to the low-gain antenna. Its resolution is about the same as that of channel 213. It has the same temperature stability problem as channels 210 and 213, and was also poorly calibrated as a function of temperature.

(6) Status, channel 301 (0-4.5 V). Channel 301 is a digital status channel and indicates the FTS data mode (engr only, RTS-1,

RTS-2, playback), the TWTA power mode (high/low power), and the ranging channel on/off status. The TWTA mode and ranging channel on/off are RFS functions. The ranging on/off status is required; however, six other telemetry channels, as well as the received signal strength at the ground station, give indications of high or low power. This channel is not normally important as a power indicator, but since it is an easily mechanized channel, it could be useful during a TWT failure.

(7) TWTA second anode voltage, channel 302 (0-3 V). Channel 302 indicates the second anode voltage of the TWTA. The telemetry voltage for each TWTA has a different center range, so that the channel also indicates which TWT is on. The value of monitoring the second anode voltage is limited, but since this voltage is an indirect measurement of the regulated +20 V dc of the TWTA, it is of some importance. This voltage is also used to generate more critical tube voltages such as the helix voltage of about 1400 V dc.

(8) Exciter -25 V dc, channel 306 (0-3 V). Channel 306 monitors the -25 V dc supply of the exciter and also indicates which exciter is on by using different telemetry voltage ranges for each of the two exciters. This channel has limited value because the -25 V dc voltage is well regulated and the exciter will work at voltages well above or below the telemetered range of -20 to -30 V. Finally, if the exciter voltages failed, there would be no downlink signal to carry the telemetry information, and a command to switch to the other exciter would be initiated immediately, either automatically or from the ground.

(9) TWTA helix current, channel 308 (0-20 mA, converted to 0-3 V). Channel 308 monitors the TWTA helix current. This is an important parameter of the TWTA, since almost any change in the operating point of the TWTA will be reflected in the helix current (or more accurately, the beam interception current). The present resolution of the channel is about 0.17 mA per data number.

(10) Receiver VCO temperature, channel 404 (-16 to +55°C). Channel 404 monitors the receiver VCO temperature. This channel aids in the prediction of the receiver best-lock frequency, which is temperature-variable. The channel's resolution could be increased from the present 0.55°C per data number to 0.11°C to provide better measurement accuracy and hence better prediction of best-lock frequency. The channel is also used as a temperature reference for calculating the RF powers indicated by channels 210, 213, and 214.

(11) Auxiliary oscillator temperature, channel 430 (-16 to +55°C). This channel monitors the temperature of the auxiliary oscillator and aids in the prediction of the one-way downlink frequency, which is temperature-variable. Increased resolution similar to that of channel 404 (as discussed above) should result in more accurate predictions of the one-way frequency.

(12) TWTA 1 and 2 base temperatures, channels 418 and 433 (-12 to +96°C). The temperatures are sensed at the critical temperature areas near the collector of each tube. These channels, in conjunction with several others, are useful in determining TWTA performance.

(13) Local oscillator drive, channel 422 (-12 to +4 dBm, converted to 0-100 mV). Channel 422 measures the level of the ×36 output to the first mixer in the receiver.

The automatic gain control (AGC) fine channel used in MM'69 was also planned for MM'71. However, midway in the program, the channel allocation was needed for another subsystem. Thus, this channel capability was built into the MM'71 RFS but never used. The AGC fine indicates receiver input signal level as does channel 115, but its range covers -130 dBm to threshold. Typically, this channel is noisy and hard to read as well as difficult to calibrate accurately. Its usefulness, as it is now mechanized, is questionable.

A telemetry relay module is common to both exciters. It conditions the composite telemetry signal before it reaches the phase modulators and also switches between two telemetry functions, depending on which exciter

is on. One of these switched functions is a monitor of the dc power supply voltage (channel 306). The other switched function is the temperature transducer located on each of the auxiliary oscillator modules. The temperature of the ON module is telemetered.

V. RFS COMMANDS

Commands are required to select the redundant capabilities (TWTAs and exciters) of the RFS, TWTA low or high power, and high-gain or low-gain antenna, and to switch ranging on and off. These commands can be direct commands from the ground stations or they can be programmed into the spacecraft CC&S, which will then command the RFS at a prescribed time. The RFS will respond to seven direct commands and five CC&S commands, as listed in Table 4.

As shown in Table 4, three of the direct commands are toggles. This type of command is undesirable, particularly for the DC-7 (switch TWTAs) and DC-8 (switch exciters), because the mechanization of the command will, under abnormal circumstances, permit the controlling relay in the RFS to "hang up" in a neutral position. If this occurs, there is no downlink. This condition cannot be corrected from the ground, and would result in loss of the mission. The TWTA control relay has hung up in the neutral position at least four times during subsystem tests as a result of spurious signals generated by turning the support equipment (SE) off with the RFS still connected. During flight operations, observation of minimum time intervals between RFS direct commands or CC&S-controlled operations is required to preclude the possibility of hangups. It is recommended that these toggle commands be avoided in future programs.

VI. RFS SUBASSEMBLIES

A. Receiver and Diplexer Subassembly

The receiver and diplexer subassembly (see Fig. 3) form the narrow-band, double-conversion, automatic phase and frequency tracking RFS receiver. When the receiver is phase-locked to the transmitted uplink signal, it supplies an output frequency to the exciter which is phase- and

frequency-coherent to the received signal. The exciter multiplies the receiver output frequency and phase by 120 for transmission at S-band. In this mode, the receiver and exciter form the transponder, which coherently translates the frequency and phase of the received signal by a fixed ratio of 240 to 221. The transponder provides for coherent two-way doppler tracking of the spacecraft, which permits accurate determination of the spacecraft trajectory. When the receiver is phase-locked to a received uplink signal which has been phase-modulated with the composite command subcarrier, the receiver demodulates the signal and sends the output to the command subsystem for direct or delayed commanding of the spacecraft. The receiver also demodulates from the uplink signal the pseudo-random noise ranging code, amplifies and limits it, and sends it to the exciter to be modulated on the downlink carrier. The ranging capability permits precise measurement of the distance from the ground station to the spacecraft.

The receiver performance characteristics comprise the first seven items listed in Table 1, and the receiver block diagram is shown in Fig. 3. The receiver has a self-contained power supply, which converts the spacecraft 2.4-kHz power to the ±15 V dc required by the receiver. The supply also provides a voltage to the first stages of the video amplifier module in the ranging channel. This voltage is turned on or off by a DC-9 command, and off by a CC&S cyclic 2A. Turning the ranging channel off by a 2A is a safeguard carried over from previous programs. With the ranging channel on, feedback onto the phase-locked loop (PLL) has sometimes created self-lock on past programs. Self-lock can cause performance degradation or a complete loss of command and two-way tracking capabilities.

Nine of the eleven receiver modules, as listed in Table 3, were modified or changed from the MM'69 configuration. However, these modifications did not require a major circuit layout change in any of the main modules. The primary reasons for the changes were to increase reliability, improve circuit stability, and reduce electromagnetic interference (EMI) and undesired signals. The latter were major contributors to self-lock and false-lock problems encountered on MM'69. As a result of these changes and those in the exciter subassembly, there was no evidence of self-lock or false lock on the MM'71 RFS.

In addition, the loop filter was completely redesigned by incorporation of a dc amplifier to increase receiver loop gain by 10. The loop gain was increased to lower the static phase error (SPE) resulting from orbital doppler from the phase detector. Minimizing the SPE reduces the probability of dropping RFS lock and/or flight command subsystem (FCS) lock. Without the increased loop gain, the uplink frequency would have to be adjusted several times during orbit to keep the SPE within required limits.

B. Exciter Subassembly

The exciter subassembly consists of two identical and fully redundant S-band exciters. The output power of each exciter is divided in half by the hybrid filter and presented to the input of both redundant TWTAs. Thus, the exciters and TWTAs provide a fully redundant transmitter chain. The exciters are phase-modulated by the composite telemetry signal for transmission of scientific and engineering information from the spacecraft. Figure 4 shows a block diagram of an exciter.

1. Design modifications for improved performance. The RFS exciter represents a complete redesign of the Mariner '69 design, although the functional operation is similar. The MM'69 ×24 frequency multiplier was changed to a ×30 and the ×5 in the phase-modulator module to a ×4. Also, the phase modulator was redesigned, and some modifications were made in the auxiliary oscillator module. The redesign resulted in several improvements over the older system. The possibility of self-lock or false lock was greatly reduced by changing the ×5-×24 to ×4-×30. This change in multiplication order reduced the number and magnitude of undesirable harmonically related signals. The ×30 did not increase the exciter RF output level, which was marginally low on MM'69, but it did reduce the exciter alignment time by about 3 weeks. The redesign of the phase modulator improved its frequency response, modulation sensitivity, and temperature stability. It also reduced the 9.57-MHz feedthrough, which contributes to the self-lock problem. The auxiliary oscillator module was modified to improve its frequency stability and to include the VCO/AUX OSC inhibit as an umbilical function.

2. RF breakdown modifications. During the final flight-acceptance testing of the second flight system, RFS S/N 005, an RF breakdown occurred on exciter 1 as the vacuum chamber was being evacuated. The chamber

pressure at the time of breakdown was about 200 μm, and therefore, the breakdown can be classified as an ionization rather than multipacting breakdown. As a result of the breakdown, the RFS output dropped about 20 dB, and the exciter output dropped well below the threshold of its level indicator. The breakdown could be cleared and everything restored to normal by momentarily turning the exciter off. Additional pumpdowns were performed on the RFS, and the breakdown was found to be fairly repeatable between 100 and 500 μm. Pumpdowns were made with exciter two on, but it did not exhibit any evidence of breakdown.

No breakdown occurred on the first flight system during its acceptance testing, although a loss in exciter power was experienced once on the PTM during vacuum chamber pumpdown. However, no power loss was detected on subsequent pumpdowns, and the cause of the power loss was never found; it was most likely the result of an RF breakdown. From this, one could conclude that the RF breakdown margin on the existing design was extremely small or nonexistent.

Although the breakdown could be extinguished by sending a command to switch exciters, it was completely unacceptable from an operational and reliability standpoint. Therefore, even though it was extremely late in the program, it was necessary to initiate an investigation to find the cause of the breakdown and take corrective steps to prevent its recurrence. This investigation caused a shortage of radio assemblies during spacecraft system testing, and the available RFS had to be moved from spacecraft to spacecraft.

As a result of the investigation, it was determined that the observed breakdown occurred in the helical filter of the ×30. A block diagram of the ×30 is shown in Fig. 5. The helical filter is a three-pole filter in the output of the ×5 frequency multiplier within the ×30. The ×5 is a varactor multiplier and was filled with foam (Nopcofoam A-206) for structural purposes only. As the investigation progressed, it was determined that the voltage breakdown margin of the ×5 without foam was very small or nonexistent under conditions of design value carrier frequency and power level. In addition, RF voltage measurements were made in the ×5 circuit and breakdown tests performed on variable capacitors used in the ×5. These tests indicated that the breakdown margin of two capacitors was insufficient.

The investigation had uncovered a number of problems which required solutions, and several were proposed or tried. One obvious solution to the RF breakdown at low pressures was to pressurize the X30 and prevent its exposure to low pressure. This approach required a complete redesign of the exciter subassembly housing, and the available space for a pressurized container was uncomfortably tight. More significant, the ability of such a container to hold its pressure for the duration of the mission was in question. Also, there was insufficient time to adequately leak-test a pressurized X30 container prior to launch. Furthermore, the pressure could bleed down and remain in the critical region where the X30 is most susceptible to breakdown. Although there were several undesirable aspects to the pressure approach, its design was completed for use if all other approaches failed.

Launching the spacecraft with the radio off was not an acceptable solution; therefore, an attempt was made to prevent the RF breakdown without pressurization. A series of possible modifications were tried on the helical filter. Holes were drilled in the filter to provide rapid venting. The breakdown still occurred, but more important, it did not extinguish when exposed to hard vacuum because of local outgassing caused by heating. Thus, this method had to be discarded. Another modification was to fill the filter with a closed-cell foam (Nopcofoam A-206). Tests showed that this raised the power required for breakdown, but it was unacceptable because (1) foamed filters were found to contain voids and nonuniform bubble size; and (2) the trapped gas in the foam cells may leak out and the cells eventually reach critical pressure. Thus, the equipment may be exposed to critical pressure and be most susceptible to RF breakdown some time after exposure to hard vacuum.

Small, hollow, silicon dioxide spheres (Emerson & Cummings Ecco Spheres SI) placed in the helical filter were found to significantly raise the power required for RF breakdown. The spheres, or "white sand," vary in diameter from 0.0254 to 0.0102 mm. These dimensions were so small that the free electrons excited by the RF field collided with the walls prior to attaining adequate energy to ionize gas internal or external to the spheres. Although the white sand provided an adequate RF breakdown margin, it was still unacceptable because it was found to settle continuously during vibration, leaving undesirable voids. At this point, "pink sand" (white sand

coated with thermosetting epoxy) was tried. This material (3M #XR5068) also provided an acceptable RF breakdown margin, and it did not settle continuously during vibration like white sand. In addition, once cured at an elevated temperature, the pink sand was no longer free to move.

During the testing, it had been determined that the X5 would break down without foam. The foam in this area was unacceptable because prior testing had shown voids in the foam and indicated possible outgassing problems. As a result, pink sand (rather than foam) was used as a breakdown suppressant in the X5. To accommodate pink sand, the mechanical design of the X5 had to be modified to incorporate a bolt-on lid and a fill hole.

As previously noted, the RF breakdown voltage margin on two tuning capacitors in the X5 was found to be marginal. To solve this problem, a fixed capacitor was added in series with each of the two tuning capacitors, which reduced the voltage across the variable capacitor to an acceptable level.

During the capacitor tests, it was determined that the O-ring seal on the rotor screw, used to keep contamination out, trapped gas inside the capacitor. Calculations show that this seal would prevent the inside of the capacitor from reaching critical pressure for about 10 days after exposure to hard vacuum. Thus, a standard capacitor could not be tested in a reasonable time frame. To expedite testing, a hole was bored in the rotor screw head. Capacitors without O-rings were ordered and installed in the flight equipment where permitted by delivery schedules.

Throughout most of the breakdown testing, an isotope source was used where feasible to produce the free electrons necessary for breakdown. If breakdown did not occur with the source in place, the possibility of a future breakdown was extremely small. RF breakdown data as a function of pressure, voltage, frequency, and spacing obtained during the various tests correspond quite well with values published by R. Woo.[1] Woo's data also provided an insight into the pressure regions deserving close examination and air gaps which should be avoided. The variable air gaps created by tuning adjustment in the X30 were carefully measured, and the critical regions were avoided.

[1]Woo, R., Final Report on RF Breakdown in Coaxial Transmission Lines, JPL Technical Report 32-1500, October 1, 1970.

As a result of the above changes, the possibility of RF breakdown in the ×30 was virtually eliminated. This was assured by first breakdown testing the various subassemblies of the ×30 at higher levels than those encountered when the ×30 is operating as a module. In general, the helical filter, the ×5, and the ×3 were tested at 6 dB above their nominal input power. The load isolator was tested as part of the ×3. The power amplifier and ×2 frequency multiplier (PA×2) output power was tested at about 3 dB above nominal by raising its dc input voltage. At the conclusion of the individual tests, the ×30 was assembled and tested for breakdown as a complete module. The breakdown testing of the ×30 included raising the dc input voltage, which increased the RF output power, and therefore the possibility of RF breakdown; no breakdown was observed.

The addition of pink sand did eliminate the possibility of both corona and multipacting breakdown in the ×30; however, the pink sand created other problems which had to be overcome. The sand could not be merely poured in the helical filter and ×5 because it would settle during vibration and leave voids. To avoid the formation of voids during RFS system vibration, it was necessary to fill the helical filter and ×5 under vibration with a prescribed amount of pink sand which had been determined experimentally. The pink sand spheres being small, the sand was hard to contain and required that all mechanical interfaces be filled with epoxy. The dielectric constant of the pink sand shifted the center frequency of the helical filter by 90 MHz compared to air. The frequency shift was corrected by tuning the filter 90 MHz above the desired center frequency prior to filling it with pink sand. A minor realignment was then performed to meet the required bandwidth and VSWR. The loss tangent of the sand also increased the loss of the filter by about 1 dB. This was compensated for by increasing the output of the PA×2. The addition of the sand also tended to increase the loss in the ×5 up to a maximum of 1.35 dB. In general, the power output of the ×30 was lower after the modification, and its temperature performance was somewhat compromised. The final ×30 performance is compared to the MM'69 ×24 performance in Table 5. During the ×30 breakdown investigation, a MM'69 residual ×24 was breakdown tested; it was found to be marginal. It is most

significant that the addition of the sand did not in any way increase the tendency for self-lock or false lock in the RFS.

C. Control Unit

The control unit accepts direct commands from the FCS, the CC&S, and the failure-sensing circuits in the RFS. It selects the appropriate RFS operating mode. The functions of the control unit are to

(1) Control the circulator switches to direct the output from either TWTA to the high-gain or low-gain antenna upon receipt of a suitable command from the FCS or CC&S.

(2) Sense the TWTA and exciter power level and, if it is low, switch to the redundant unit upon receipt of the CC&S 2A cyclic command.

(3) Sense overcurrent conditions in the TWTA and exciter power supplies and switch immediately to the redundant unit; switch to either redundant element upon receipt of a direct command from the FCS.

(4) Select high or low power output from the TWTA upon receipt of a command from the FCS or the CC&S.

(5) Sense overcurrent in the receiver power supply and remove its prime power if such a condition exists. The prime power is reapplied to the receiver upon receipt of each subsequent CC&S 2A cyclic command.

The control unit consists of 16 welded, encapsulated corwood modules and five magnetic latching relays. The latching relays provide memory, efficient switching and control, as well as isolation between functions.

The MM'71 control unit is basically a MM'69 design with some modifications. A block diagram of the control unit is shown in Fig. 6. In MM'71, the CC&S command 2B, transmit low-gain antenna, was added, and a change was required in the control unit to implement this command. The antenna switching logic was changed to prevent, where possible, high RF energy from the ON TWTA from being fed into the OFF TWTA. The MM'69 design of the constant-current driver for the circulator switch did not meet MM'71 temperature specifications. In addition, the switch current was raised from

the MM'69 value of 15 mA to 22 mA for MM'71. A circuit modification eliminated both of the deficiencies. Redundant zener diodes were added to the two redundant power supplies in the exciter level sensor supply as recommended by the MM'69 program.

D. Traveling Wave Tube Amplifiers

The TWTAs consist of two TWTs, each with its encapsulated, modular, solid-state power supply. The block diagram for one TWTA is shown in Fig. 7, and major performance parameters are presented in Table 6.

The TWTA functions as a power amplifier of the phase-modulated S-band signal from the exciter. It provides two output power levels, nominally 10 or 20 W, by changing the voltages applied to the TWT helix, collector, and first anode. The MM'71 TWTA is essentially the same as that used in MM'69.

The TWTA procurement involved two separate contractors. The TWTs were purchased on a fixed-price contract by JPL from one contractor. The tubes were then supplied to the second contractor, who mated the TWT with his power supply and performed the acceptance testing on the TWTA. The second contract was also fixed-price. This procurement technique did present some minor contractual problems and should probably be avoided in the future.

During the MM'69 program, noise and ripple voltage appeared on the dc primary lines of some TWTAs at certain temperatures and line voltages. This voltage was generated in the voltage regulator module as a result of instability in the feedback loop regulating the output voltage. An attempt was made on the MM'71 program to correct this problem. However, the solution was not entirely successful, and some noise continued to appear on the dc primary lines. The noise was still a function of input voltage and temperature. In addition, the solution was incorporated only in the TWTAs that required rework. While the noise has not been found to be a reliability problem or degrade the TWTA or RFS performance, it is annoying and exceeds specification limits. Furthermore, it represents an unstable condition, and there is some concern that the noise could increase to the point of degrading the TWTA performance. Elimination of the instability is recommended for future programs.

During preflight testing, one TWTA developed a short in the high-voltage converter (HVC) between a high-voltage transformer and an anodized plate connected to the chassis. Analysis of the failure indicated that there was insufficient spacing between the transformer and plate. This was corrected by increased spacing, and the solution was eventually incorporated into three of the four flight units. However, this solution may not be optimal, and additional design effort on the HVC should be considered by future programs. Also, in the present TWTA design, the high-voltage transformers are potted into the HVC and cannot be removed. This means that the HVC must be changed when the TWT is replaced with one that requires a different voltage. Some consideration should be given by future programs to making the transformer more accessible to improve the TWTA repairability and make TWT changes less costly in both time and money.

Initially, the MM'71 program was scheduled to use only residual MM'69 TWTs, and thus, no procurement for new tubes was planned. However, after one tube had gone to air, and since good spare tubes were nonexistent, it was decided to purchase additional TWTs. The undesirable idiosyncrasies of the existing tubes scheduled for flight had a significant influence on this decision. Also, it was getting so late in the program that a later procurement would not allow for the time required to build new tubes and meet the launch dates. The decision to purchase additional tubes at that time proved to be a good one.

The TWT contractor strongly recommended that the design of the output window assembly and collector be changed on the new tubes. The proposed design change had been successfully used on similar TWTs. The change would significantly reduce the stress per unit area on the ceramic insulator between the tube body and collector and thereby increase the reliability of the TWT. Two TWTs, one in MM'69 and one in MM'71, had developed leaks and went to air as a result of a crack in the old insulator design. The new design would reduce the possibility of a recurrence of this defect. The new collector design, a bucket type, would reduce backstreaming electrons by reducing the number of secondary and primary electrons that escape the collector. These design changes were incorporated into the new tubes, which were designed as an HAC 242 HA; the old design was an HAC 242 H. The new tubes were subjected to a flight-acceptance

vibration test at the contractor's plant. This test was performed with power applied to the tube; in the case of MM'69 power was off during the vibration test. In addition, the MM'71 vibration levels were tailored to match those encountered in the RFS bay during assembly level vibration. As a result, the MM'71 vibration levels used at the vendor during acceptance testing were higher than those used for MM'69.

As a result of the design changes, the helix current was decreased, which improved the efficiency of the TWT. Also, the amount of "hiccupping" (a quasi-periodic variation in helix current and/or power output) and helix current steps were significantly reduced in the new tubes.

As the MM'71 program progressed, it was necessary to replace two TWTs in addition to the one which had previously gone to air, each with an HAC 242 HA. One tube was changed because its turn-on characteristics were abnormal. During tests performed on this tube after the change, a collector-to-helix short developed, preventing further analysis. It is not known whether this short was related to the abnormal turn-on characteristics. The other TWT was changed because it began to exhibit periodic phase transients during a thermal vacuum test. Analysis revealed a broken wire in the tube's output connector assembly; the break was external to the vacuum envelope.

E. Microwave Components

The microwave components consist of the hybrid filter, output filters, RF switch, and diplexer. The electrical characteristics of the microwave components are shown in Table 7. Stripline on polyphenelene oxide (PPO) construction is used for the hybrid, the switch, and all power monitors. Coaxial cavities are used in the other circuits. Some changes were made to all of the microwave components except for the output filter during the MM'71 program.

1. General component modifications. The most significant difference between the MM'69 and MM'71 microwave component design lies in the RF switch, which will be discussed later. In the MM'69 design, the voltage rating of the level sensor and telemetry diodes in the various units was too low. In MM'71, higher-voltage diodes were used in all level sensor and telemetry circuits, which solved previously encountered problems.

The circuit boards in some of the residual MM'69 hardware were found to be cracked and crazed for undetermined reasons. To protect against a possible trace failure due to the cracked PPO boards, a trace was placed on the backup board. Thus, the circuit boards which faced each other both contained a trace, one being the mirror image of the other.

Patches of mylar tape were used between the trace and tuning screws in the MM'69 design. The MM'71 program replaced the tape with mylar discs, which was necessary to accommodate the dual trace. The disks were installed by placing them into the tuning screw hold after the switch was assembled. In MM'71, ferrite beads were added to the level sensor and telemetry leads, which eliminated the EMI susceptibility encountered in MM'69.

2. Hybrid filter. The hybrid filter divides the power output from each exciter and furnishes drive power to both TWTs simultaneously through band-pass filters. Attenuators are used in the hybrid filter input and output circuits to adjust the exciter drive to an optimum value for each TWTA, and to compensate for hybrid filter imbalance.

3. Output filter. The output filter is used in the TWTA output circuit. It has minimum insertion loss at transmitter frequencies, a band-reject filter at receiver frequencies, and a low-pass filter to attenuate transmitter output harmonics.

4. RF switch. The RF switch consists of two circulators, making a four-port circulator switch. It provides a means of connecting either TWTA to the high-gain or the low-gain antenna. A permanent magnet assures that TWTA 2 will be connected to the high-gain antenna, with about 3.5 dB power loss, in case the switch coil voltage supply fails. Failure sensing for the TWTA outputs is accomplished at the input to each circulator, and the high-gain antenna telemetry power monitor is at the HGA output of the switch.

The RF switch in the MM'71 RFS was initially scheduled for minor design changes from the MM'69 baseline design, consisting primarily of the addition of the dual trace and ferrite beads, as previously noted. However, a switch problem, which resulted in additional design changes, was uncovered at the system contractor's facility during the PTM RFS thermal

vacuum test. The output power from the RFS, and thus switch loss, was found to be a direct function of atmospheric pressure. The RF output power started to drop in the vicinity of 1000 μm and continued to decrease as the pressure was reduced. At a pressure of 1.332×10^{-6} N/cm^2 (10^{-4} torr), the RF output, depending on the radio mode, had degraded by 1 to 2 dB. Also, when antennas or TWTAs were switched, the RF output power would rise to its normal level and then decay within 5 s to its degraded value in a vacuum environment. When the RFS was returned to room pressure, the RF output power returned to its normal value. The PTM switch was returned to JPL, and the reduction in RF power output was duplicated in vacuum tests. To verify a potential design deficiency, the Flight 1 switch, which was identical with the PTM unit, was subjected to a vacuum test; it exhibited the same breakdown anomaly as the PTM. The power loss was identified as a RF breakdown between the tuning screws and the trace.

As a result of inadequate testing techniques, the RF breakdown was not discovered by the switch contractor during vacuum acceptance tests. This situation must be corrected on future programs by improving test techniques and procedures.

The MM'71 switch differed from the MM'69 switch in two respects which reduced the RF breakdown margin: (1) The MM'71 switch used a dual trace concept. (2) Mylar disks 0.076 mm (0.003 in.) thick and 4.445 mm (0.175 in.) in diameter where placed under each tuning screw in place of the patch of mylar tape as used in MM'69. The location of the mylar disks depended upon the boards being in firm contact to avoid their migrating. A gap greater than 0.076 mm would allow the disk to migrate.

The prototype switch, which had not been changed from MM'69 design, was successfully vacuum tested at a power level of 22 W at JPL. The PTM switch was converted back to the MM'69 design, i.e., single trace and mylar tape over the trace. When vacuum tested, the PTM exhibited momentary breakdowns at 22 and 30 W. It is interesting to note that the switch did recover and successfully withstood 44 W. Thus, it was determined that the breakdown safety margin of the MM'69 design was unacceptable.

A program was established in which the switch contractor was to analyze the problem and produce a satisfactory solution. Concurrently, JPL set up a parallel program to accelerate the solution. As the program

progressed, JPL assumed more of the task load while the contractor implemented each JPL-originated improvement into the PTM switch.

The power loss in the switch was identified as a RF breakdown between the tuning screws and the trace. To simplify the implementation of the JPL investigation, a stripline test fixture was used to explore the breakdown region for possible design changes. The test fixture was representative of the stripline circuit employed in the switch. It was soon recognized that the addition of the trace on the backup board increased the possibility of breakdown between the tuning screw edge and the added trace. The tuning screw passed directly through the trace with insufficient radial clearance.

To provide a greater safety margin, disks of thin K-15, a high dielectric material, were introduced between the tuning screw and the trace. These disks were larger in diameter than the tuning screw in the PPO backup board and were held in position by a counter bore in the backup PPO. This change was incorporated into the PTM switch. The switch was vacuum tested, and breakdown did not occur until the power level reached 46 W. The breakdown occurred between the surface of the K-15 and the tuning screw.

Data published by R. Woo (see footnote 1) indicate that breakdown will occur with 45 W of incident power when the frequency and spacing (f-d products) between electrodes is between 70 and 175 MHz-cm. This represents a spacing of 0.305 to 0.76 mm (0.012 to 0.030 in.) at 2300 MHz between the K-15 and tuning screw. In tests performed, breakdown occurred at 45 W, with gaps lying between 0.279 and 0.635 mm (0.011 and 0.025 in.). To assure that the switch would exhibit an acceptable breakdown margin, tuning screw gaps between 0.127 and 1.016 mm were avoided by filling the gaps with thin teflon disks about 1.5 times the thickness of the gap and the same diameter as the tuning screw hole in the PPO board. By eliminating the 0.127- to 1.016-mm (0.005- to 0.040-in.) air gap, the f-d range of 29 to 234 was excluded. According to Woo, this would permit the screw gap to handle about 70 W of incident power at the spacecraft transmitter frequency.

A total of 12 stripline fixture tests were performed using a combination of K-15 and teflon, reducing the 0.127- to 1.016-mm air gaps to less than 0.127 mm. The fixture was vacuum tested at 50 W without any RF breakdowns. The available test equipment would not permit testing at a higher power level.

The technique of excluding the critical air gaps by the use of teflon was applied to the PTM switch. The switch was tuned up, and all gaps were carefully measured. Eight of the 19 gaps were found to lie between 0.127 and 1.016 mm; these were filled with teflon to reduce the air gap to less than 0.127 mm. The PTM switch was vacuum tested in all modes at powers up to 45 W, and no breakdown occurred. Potential contractual and schedule problems prevented testing the switch to a higher power.

The two flight switches were retrofitted with K-15 and teflon. The switch contract specified the acceptance testing to be performed at 30 W, and therefore the flight switches could not be vacuum tested at a higher level. Both flight switches successfully passed the 30-W tests. It is recommended for future programs that the test level be raised to a minimum of 60 W. This would provide about a 5-dB margin when the TWTA is operating in the high-power mode.

A second switch problem was uncovered late in the MM'71 program. The Flight 2 switch began to exhibit a new anomaly: when the switch was operated to shift from the high-gain to the low-gain antenna, an increase of 1 dB in insertion loss was observed. This malfunction occurred over a limited temperature range and could also be induced by the application of a mild mechanical pressure in the vicinity of the ferrite junction area.

Disassembly of the unit revealed an intermittent circular contact between one ferrite subassembly and the stripline junction trace. It was determined that dimensional tolerance buildup resulted in insufficient pressure contact and the ferrite subassembly was not securely held to the trace. A procedure was established by the contractor to select parts to provide, in the final assembly, sufficient pressure to ensure continuous contact around the periphery of the ferrite subassembly with the stripline trace.

5. Diplexer. The diplexer provides a band-reject filter at receiver frequencies between the transmitter output (RF switch) and the low-gain antenna, with a band-pass filter at receiver frequency and a low-pass filter between the low-gain antenna and receiver (first mixer) input. Also, the low-gain antenna telemetry power monitor is contained in the diplexer.

VII. RFS PERFORMANCE AND TEST HISTORY

The purpose of the tests performed on the RFS by the subsystem contractor and JPL was to determine the flight readiness of the RFS as part of the spacecraft system and its compatibility with other subsystems and the System Test Complex. In addition, operating procedures were verified and personnel was trained.

In general, testing was performed at the module, subassembly, and RFS levels by the subsystem contractor. At JPL, the RFS was tested alone and in the spacecraft system; it was retested at module, subassembly, and RFS levels after rework. At the Air Force Eastern Test Range (AFETR), it was tested alone and in the spacecraft.

A. Contractor Tests

At the contractor's plant, the modules were aligned and bench tested, then conformally coated, readjusted, and acceptance tested. Next subassembly (i.e., receiver and exciter) tests were run, followed by the overall RFS assembly testing.

Test limits for flight acceptance (FA) were more severe than the anticipated environment in flight, and the type acceptance (TA) limits on the PTM were still more severe. Modules and major subassemblies were tested to FA (flight) or TA (PTM) temperatures at ambient air pressure, and the complete RFS was tested in a vacuum. The MM'71 temperature range was 0 to 55°C for FA and -20 to +75°C for TA (the same as MM'69). However, the flight receiver and exciter subassemblies and their modules were tested to 60°C at the subsystem contractor, and the flight TWTA's were acceptance tested, by the TWTA contractor, to 75°C as measured on the TWT base plate.

B. JPL Receiving Tests

As each RFS was received, it was subjected to verification tests to assure that no damage had occurred in shipment. The system was taken to the telecommunications development laboratory (TDL), where it was interfaced with the command and telemetry subsystems and the modulation index was adjusted if necessary. Bit error rate tests were also run on the three systems after they were interfaced, and the TDL test complex was also used

for miscellaneous RFS tests. After verification and calibration of the subsystem test complex equipment system performance, power output, and cable losses, the SE/RFS compatibility was verified and the initial checkout of the RFS was performed before it was mounted on the spacecraft.

C. Spacecraft/RFS Integration Tests

The spacecraft/RFS integration test achieved the following objectives:

(1) Verification of spacecraft/RFS mission test computer (MTC) interfaces and of interfaces with other subsystems.

(2) Measurement of the RFS power profile.

(3) Determination of the functional capability of the RFS as part of the spacecraft.

(4) Verification of RFS/DSIF compatibility as measured by the Compatibility Test Area (CTA-21), DSIF station at JPL.

(5) Determination of the operational readiness of the RFS SE and its interfaces with the system test complex.

D. Subsystem Tests

The objectives of the subsystem test were the evaluation of the performance of the RFS while operating with spacecraft power and in the system environment, and to make a preliminary determination of any possible effects of the RFS on the system environment. The subsystem tests included all mission-required modes and determined the ability of the RFS to perform according to its functional and design requirements. Variations of performance and interaction effects of the subsystem and the spacecraft were evaluated. Parameter variation tests were run to determine performance margins, and power profiles were measured.

E. Spacecraft/RFS Mission Compatibility Tests

The spacecraft/RFS mission compatibility tests demonstrated that spacecraft and DSN telemetry and command data systems met mission requirements, that the ground system and personnel could operate the spacecraft satisfactorily, and that the flight telecommunications systems and the DSIF were compatible.

After verification of all subsystems and interfaces, the mission tests were conducted. These tests included simulated launch, separation, acquisition, cruise, and playback, under hot and cold vacuum conditions. Engineering and command exercises were performed with attitude control and midcourse maneuvers and science exercises.

F. Electromagnetic Interference Tests

Electromagnetic interference tests were conducted on all flight models. The tests consisted primarily of subjecting the spacecraft to an electromagnetic field simulating launch conditions.

At JPL, RF power was radiated into the spacecraft and also connected to the low-gain antenna port. The levels used for this test were intended to be 6 dB higher than those expected from the launch vehicle. The PTM was found to be susceptible to these levels when the ranging channel was on, causing a reaction in the AGC and SPE. The spacecraft is launched with ranging off, and therefore this was not a serious problem.

At AFETR, only radiated power was used for the EMI test. No problems were experienced with any RFS during this test, nor were any EMI problems caused by the launch vehicle telemetry systems.

During the RFS Flight 1 bench and alignment test at the subsystem contractor, the receiver exhibited the same general characteristic as during the EMI test at JPL. The condition existed for only about 1/2 h and could never be repeated. It was most likely caused by an unknown EMI source.

G. DSIF Compatibility Tests

The objective of the DSIF compatibility tests with CTA-21 was to demonstrate functional and operational compatibility among all interfacing elements of the spacecraft and the DSIF. A calibrated S-band link was provided between the spacecraft in the Spacecraft Assembly Facility (SAF) and the CTA-21 receiver exciter ranging (RER) subsystem, with additional hardlines to provide a source of data for bit error rate measurement. Calibrated attenuators in the simulated uplink and downlink signal paths provided known signal levels from threshold to -90 dBm at the receiver diplexer input and the DSIF receiver low-noise amplifier input.

After interface checkout and calibration of all elements of the system, and with the spacecraft in cruise mode, the RFS best-lock frequency was verified, and the spacecraft receiver threshold was measured. Then, with the spacecraft in science and playback mode, the best-lock and threshold measurements were repeated. These measurements were made with the RFS in various modes to verify the performance of redundant elements and of the high- and low-gain antennas. Ranging and command performance were also verified. Tracking and acquisition capabilities were determined, spectrum analyses were performed, and auxiliary oscillator frequencies and phase jitter were measured. The effects of SPE offsets and ranging modulation on the spacecraft command capability were also measured. The test results indicated that the RFS was compatible with the DSIF and capable of meeting the mission requirements.

H. Miscellaneous Tests

Vibration, weight and center of gravity, acoustic, simulated launch complex, electromagnetic interference, and pyrotechnic shock tests were performed on each spacecraft. However, because of a schedule conflict caused primarily by the exciter RF breakdown problem, RFS S/N 003 did not receive the spacecraft vibration test.

I. Recommendations for Improvements in Testing

1. Test team staffing. Test teams for the MM'71 program generally consisted of two men per subsystem, with one man being a full-time operator and the second splitting his time between operating and data analysis. The second man also devised tests to resolve anomalous performance and provided data necessary to close problem failure reports (PFRs). This system worked quite well but does not provide adequate manpower for long-term test such as thermal vacuum. In addition, during periods of high activity, the two-man team was inadequate for real-time data analysis, which had to be performed by non-team personnel. Real-time analysis has proved to be one of the most useful tools for detecting anomalous performance.

2. Data logging. In MM'71, an oscillograph recorder was used to analog-record several RFS direct-access or telemetry functions. This recorder was used for RFS assembly-level testing at the contractor, and

during system test at JPL and AFETR. The recording was analyzed on a near-real-time basis. This method of data analysis is time-consuming, but it has proved to be extremely worthwhile for the early detection of anomalous performance or change in RFS signature.

Neither previous programs nor MM'71 have made use of a data acquisition system for analog-recording direct-access functions and selected SE functions. In MM'71, a great deal of time was spent in manually recording data. This time could be more wisely spent in analyzing automatically recorded data. It is recommended that a data acquisition system be used on future programs. However, it will not replace the oscillograph recorder because it will not record transients.

3. Data retrieval. Typically, many problems of anomalous performance recur and warrant a speedy review of old test data. In MM'69, the system for data identification, storage, and retrieval was almost nonexistent. A big improvement was made in MM'71 in that all RFS data, including the numerous rolls of oscillograph recordings, were identified, cataloged, and stored in a designated area. This sytem worked quite well and was well worth the effort, but could be improved upon by a closer to real-time identification and cataloging of data.

4. Calibration. Accurate prediction of auxiliary oscillator (downlink) and best-lock (uplink) frequencies is particularly desirable during a mission. Accurate knowledge of telemetry data is also valuable in the daily assessment of system performance and in the recognition and evaluation of any anomalous in-flight performance. Both of these items require accurate temperature calibration of the telemetry channels. Several of the RFS channels, namely 111, 115, 210, 213, and 214 (see Section IV for description and details) are temperature-dependent, and thus particular attention must be given to the temperature at the time of calibration. In flight, the temperature-sensitive channels use the VCO temperature as a reference. Unfortunately, the MM'71 test procedures did not always require the VCO temperature to be noted at the time the temperature-sensitive channels were calibrated. This oversight must be corrected on future programs. An additional improvement in the calibration of the transmitter power channels could be made if temperature transducers were located next to the diode detectors. To be useful in flight, this would require three additional

temperature channels, one for each diode detector. The number of additional channels could be minimized by more efficient utilization of existing temperature channels. For instance, the TWT temperature channels could be combined into one by switching to the transducer of the ON TWTA.

The MM'69 and the MM'71 RFS were calibrated at only three temperatures, typically 25° C and the FA limits. It is recommended that the calibrations be made at five temperatures: one centered at the expected flight temperature, one at each extreme of the expected range, and the other two at the FA limits. Both VCO and AUX OSC temperatures should be noted at the time of calibration. The best time to make or verify previous calibrations is during systems thermal vacuum when the spacecraft is closest to its intended space environment.

J. AFETR Tests

At AFETR, special tests were run to verify that the spacecraft was not damaged in transit from JPL. The test was divided into four parts: (1) a preliminary test including special tests that could not be done during the normal testing sequence, (2) a detailed examination of the spacecraft during an accelerated mission sequence, (3) an encounter sequence, at which time the radio was examined in detail, and (4) a playback sequence, during which the interface between the data storage subsystem (DSS), FTS, and RFS was verified.

The spacecraft was moved to the explosive safe facility (ESF) after system test at building A0. A modified system test was run with the RF link as the only command and data link. No direct access was provided. The spacecraft was encapsulated, and precountdown tests were performed.

The spacecraft was moved from the ESF to the pad and mated with the vehicle. Compatibility precountdown tests were performed between the spacecraft, launch complex equipment (LCE), launch complex, launch vehicle, Deep Space Network (DSN), and building A0. An electromagnetic interference and joint flight-acceptance composite test (J-FACT) was performed, with a precountdown test starting at T - 230 min, the spacecraft umbilical released at T = 0, and ending after verification of proper spacecraft operation. The precountdown test was conducted around a fixed

sequence of events as opposed to a rigid time sequence. A composite readiness test (based on a time sequence) was conducted, with all events occurring as they would at launch.

During testing at AFETR, several anomalies occurred. There were two instances of receiver AGC indicating the presence of an uplink signal on the RFS when none was known to be present. Investigation showed that one was caused by the Apollo tracking ship in the harbor, which saturated the receiver front end with its radar. The other occurred when DSS-71 had its transmitter on but not connected to a dummy load as intended.

When Mariner 9 was on the pad, a slight variation was discovered in the second anode voltage of TWTA 1, telemetry channel 302. The variation in voltage was most likely caused by a loose terminal on a printed circuit (PC) board, which resulted in a very low voltage on the TWT second anode; however, the operation of the TWTA was normal. The second anode acts as the ion trap in the low-power mode; the low voltage reduced the effectiveness of this trap. The first anode acts as the ion trap in the high-power mode. A constraint was placed against operation of TWTA 1 in the low-power mode, and the spacecraft was launched on TWTA 2.

The low-gain antenna drive monitor indicated a change in drive power when the antenna was connected in place of the dummy load, when the spacecraft was moved from place to place, or when there was movement of people or equipment in the vicinity of the antenna. A definite pattern was established, with fairly uniform readings observed in any one location or with the antenna off. The range of the variations was slightly more than 1 dB, with the lowest power indications occurring on the pad. These variations were attributed to the change in voltage standing wave ratio (VSWR) that took place when the antenna was installed, and to the effect of objects near the antenna coupled with inadequate directivity of the directional coupler used to sense power. Temperature effects on sensor circuit calibration tended to obscure these variations and had to be taken into account before the power output pattern could be established.

There was also an effect on the output power observed in the blockhouse caused by relative movement between the antennas on the spacecraft and the tower. This appeared at irregular intervals as a damped sinusoidal wave having a starting amplitude of up to about 0.5 dB and dying out after

6-10 cycles. The period of the sinusoid was about 1 Hz. The effect was observed on both high- and low-gain antennas and was more pronounced when there was greater activity on the tower. There appears to be no urgent reason to make design changes to reduce this effect as long as its cause and approximate magnitude are known.

Measurement of receiver threshold was difficult using the LCE with the spacecraft on the launch pad and people working in the vicinity. Threshold degradation of as much as 3 dB was observed. Possible causes for this condition are:

(1) Effects of proximity of people and equipment.

(2) Locally generated noise affecting the receiver.

(3) Excessive phase jitter in the LCE.

(4) Multipath transmission to the precision coupler via the hard-line cable and the air path to the low-gain antenna, with reflections varying according to movement of people and equipment near the antenna.

K. Miscellaneous Problems and Recommendations

Many problems were encountered in the RFS, its subassemblies, or modules during the MM'71 program, which resulted in a total of 300 PFRs prior to launch. Out of the 300 PFRs, 221 were written by the various contractors, 70 at JPL, and 9 at AFETR. For the most part, the problems were not defined as being mission-critical but were considered minor out-of-spec conditions or performance idiosyncrasies. However, some problems resulted from design deficiencies, component failures, or poor workmanship; those required corrective action.

The MM'69 program was plagued with tuning capacitor problems and initiated a program to lubricate the threads and limit the number of times the rotor could be turned before the capacitor must be replaced. This procedure was followed in MM'71 and resulted in only minor tuning capacitor problems.

In the event a module required rework, it was retested prior to installation in the subassembly. The subassembly was then retested and, finally, after it was reinstalled, the RFS was retested to bench FA limits.

Following this, except for one instance where time did not permit, the RFS was subjected to a modified FA vibration and thermal vacuum test.

Throughout the MM'71 program, the phase jitter measurements were generally out of specification because of noisy oscillators in the SE. It is recommended that the oscillator noise be reduced in future programs. The high phase noise made it difficult to accurately assess RFS performance in this area.

The bench test and TA/FA test procedures used in MM'71 required a great deal of repetitive data to be recorded, which was unnecessary. It is recommended that future programs scrutinize these procedures and reduce the amount of repetitive data taking.

Table 1. Design values of significant RFS parameters

Parameter	Value
Receiver input frequency	2115 ±5 MHz
Receiver tracking threshold	-153 dBm
Receiver tracking loop noise bandwidth at threshold	18 Hz
Command channel noise bandwidth (single-sided)	2.5 kHz
Ranging channel noise bandwidth (single-sided)	1.5 MHz
Receiver noise figure	7.5 dB
Dynamic signal level range	-70 dBm to threshold
Transmit/receive frequency ratio	240/221
Transmitter output frequency	2295 ±5 MHz
Transmitter output power	
Low-power mode	10 W
High-power mode	17 W
Telemetry and ranging channel modulation bandwidth	1.5 MHz
Power required	
2.4 kHz, 50 V	24 W
25-50 V dc TWT (high-power/low-power)	90/54 W
Weight of radio assembly	28.5 kg (63 lb)

Table 2. Radio modes

Mode	Transmit high-gain	Transmit low-gain	Exciter	Power amplifier	High-power	Low-power	Ranging channel ON/OFF	One-way	Two-way
1	OFF	ON	1	1	OFF	ON	OFF	ON	OFF
2							ON	OFF	ON
3							ON	ON	OFF
4							OFF	OFF	ON
5	ON	OFF	1	1	OFF	ON	OFF	ON	OFF
6							ON	OFF	ON
7							ON	ON	OFF
8							OFF	OFF	ON
9	OFF	ON	2	1	OFF	ON	OFF	ON	OFF
10							ON	OFF	ON
11							ON	ON	OFF
12							OFF	OFF	ON
13	ON	OFF	2	1	OFF	ON	OFF	ON	OFF
14							ON	OFF	ON
15							ON	ON	OFF
16							OFF	OFF	ON
17	OFF	ON	1	1	ON	OFF	OFF	ON	OFF
18							ON	OFF	ON
19							ON	ON	OFF
20							OFF	OFF	ON
21	ON	OFF	1	1	ON	OFF	OFF	ON	OFF
22							ON	OFF	ON
23							ON	ON	OFF
24							OFF	OFF	ON
25	OFF	ON	2	1	ON	OFF	OFF	ON	OFF
26							ON	OFF	ON
27							ON	ON	OFF
28							OFF	OFF	ON
29	ON	OFF	2	1	ON	OFF	OFF	ON	OFF
30							ON	OFF	ON
31							ON	ON	OFF
32							OFF	OFF	ON
33	OFF	ON	1	2	OFF	ON	OFF	ON	OFF
34							ON	OFF	ON
35							ON	ON	OFF
36							OFF	OFF	ON
37	ON	OFF	1	2	OFF	ON	OFF	ON	OFF
38							ON	OFF	ON
39							ON	ON	OFF
40							OFF	OFF	ON
41	OFF	ON	2	2	OFF	ON	OFF	ON	OFF
42							ON	OFF	ON
43							ON	ON	OFF
44							OFF	OFF	ON
45	ON	OFF	2	2	OFF	ON	OFF	ON	OFF
46							ON	OFF	ON
47							ON	ON	OFF
48							OFF	OFF	ON
49	OFF	ON	1	2	ON	OFF	OFF	ON	OFF
50							ON	OFF	ON
51							ON	ON	OFF
52							OFF	OFF	ON
53	ON	OFF	1	2	ON	OFF	OFF	ON	OFF
54							ON	OFF	ON
55							ON	ON	OFF
56							OFF	OFF	ON
57	OFF	ON	2	2	ON	OFF	OFF	ON	OFF
58							ON	OFF	ON
59							ON	ON	OFF
60							OFF	OFF	ON
61	ON	OFF	2	2	ON	OFF	OFF	ON	OFF
62							ON	OFF	ON
63							ON	ON	OFF
64							OFF	OFF	ON

Table 3. Design changes

Equipment	Change
Receiver subassembly	
Video amplifier	Modify circuit to reduce EMI to minimize self-lock and false lock.
×36 multiplier	Modify varactor mounting to assure electrical contact.
×1/2 multiplier	Change transformer to prevent tendency to operate as ×1/4.
AGC detector	Reduce EMI on power leads; improve reference amplifier stability.
Phase detector	Add filtering to reduce EMI; change reference amplifier from grounded base to grounded emitter to improve stability.
VCO	Add filtering to reduce EMI on power lines; modify VCO circuit to reduce parasitic oscillation.
Loop filter	Redesign to incorporate dc amplifier to increase PLL gain by 10.
Isolation amplifier and balanced detector	Improve 9.57-MHz trap to reduce 9.57-MHz feedthrough.
47.8-MHz IF	Revise output circuit to redistribute gain and provide greater linear output range; improve input VSWR.
Exciter subassembly	
Auxiliary oscillator	Add zener diode for improved stability; incorporate VCO/AUX OSC inhibit as umbilical function; improve input VSWR.
Phase modulator	Redesign; change ×5 to ×4 multiplier.
×24 multiplier	Redesign; change to Apollo-type ×30; incorporate RF breakdown suppressant.

Table 3 (contd)

Equipment	Change
Control unit	
A16 module	Add CC&S 2B capability; modify circuit to incorporate new antenna switching logic.
A12 module	Improve regulation of constant-current driver for circulator switch; increase switch current from 15 to 22 mA.
A1 and A7 modules	Add redundant zeners.
Microwave	
Isolator	Incorporate backup trace on some units; replace mylar tape covering trace under tuning screws with mylar disks (not recommended for future programs).
Hybrid filter	Change single to dual RF trace; change level sensor and TLM diodes; reduce EMI susceptibility by use of ferrite beads.
Diplexer	Change single to dual trace; change level sensor and TLM diode detector; reduce EMI susceptibility by use of ferrite beads.
Circulator switch	Change switch modes to prevent TWTA damage by high RF energy; change switch design to limit tuning screw gaps to increase breakdown margin.
Spacecraft bay VI (RF chassis)	Add heaters to maintain thermal balance when TWTA is off.

Table 4. RFS commands

Commands	Functions
Direct	
DC-7	Switch to power amplifier (toggle)
DC-8	Switch to exciters (toggle)
DC-9	Switch to ranging ON/OFF (toggle)
DC-10	Transmit low-gain antenna
DC-11	Transmit high-gain antenna
DC-42	Switch to TWT high power
DC-43	Switch to TWT low power
CC&S	
2A	Test radio
	Turn ranging channel off if on
	Reset receive overcurrent circuit breaker if tripped
	Switch to alternate exciter if exciter RF output is low
	Switch to alternate TWTA if TWTA RF output is low
2B	Transmit low-gain antenna
2C	Switch to TWTA low power
2D	Switch to TWTA high power
2E	Transmit high-gain antenna

Table 5. Electrical comparison of MM'69 ×24 and MM'71 ×30 multipliers

Parameter	MM'69 ×24	MM'71 ×30
Output frequency	2295 MHz	2295 MHz
Output power	+23.5 dBm (min.)	+23.35 dBm (min.)
Output power stability[a]	±0.5 dB	+0.5, -1.25 dB
Output bandwidth	60 MHz	90 MHz
Output frequency	95.6 MHz	76.5 MHz
RF input power	+3 ±3 dBm	+10 ±2 dBm
dc input power	6.8 W (spec.)	6.8 W (max.)

[a]Over FA temperature range.

Table 6. Typical TWTA major performance parameters

Parameter	MM'71 performance
Size, cm	24.89 × 15.24 × 19.05
Weight, kg	8.62
Input RF drive, mW	50
Power output, W	22 (high power) 11 (low power)
Overall efficiency, %	24
Power supply, V dc	25 to 50

Table 7. Microwave component electrical characteristics

	Insertion losses, dB		
	Transmit[a]	Receive[b]	Rejection
Hybrid filter	4.5[c]	>100	>100 @ dc to 2117 MHz > 60 @ 2199.8 and 2391.8 MHz >100 @ 2477 to 4000 MHz >70 @ 4000 to 10,000 MHz
Output filter	<0.3	> 60	>30 @ 2100 and 2125 MHz >70 @ 4580 to 10,000 MHz
Diplexer			
LGA to receiver	>100	<1.2	>100 @ dc to 1988.4 MHz > 70 @ 1988.4 to 2048.4 MHz
Transmitter to LGA	<0.3		
Transmitter to receiver		>50	Reverse isolation
			Minimum
RF switch			
TWTA 1 to HGA	<0.35		>25
TWTA 2 to HGA	<0.7		>50
TWTA 1 to LGA	<0.7		>50
TWTA 2 to LGA	<0.35		>25

[a]2290.2 to 2301.3 MHz.

[b]2108.7 to 2119.2 MHz.

[c]Includes 3-dB power split.

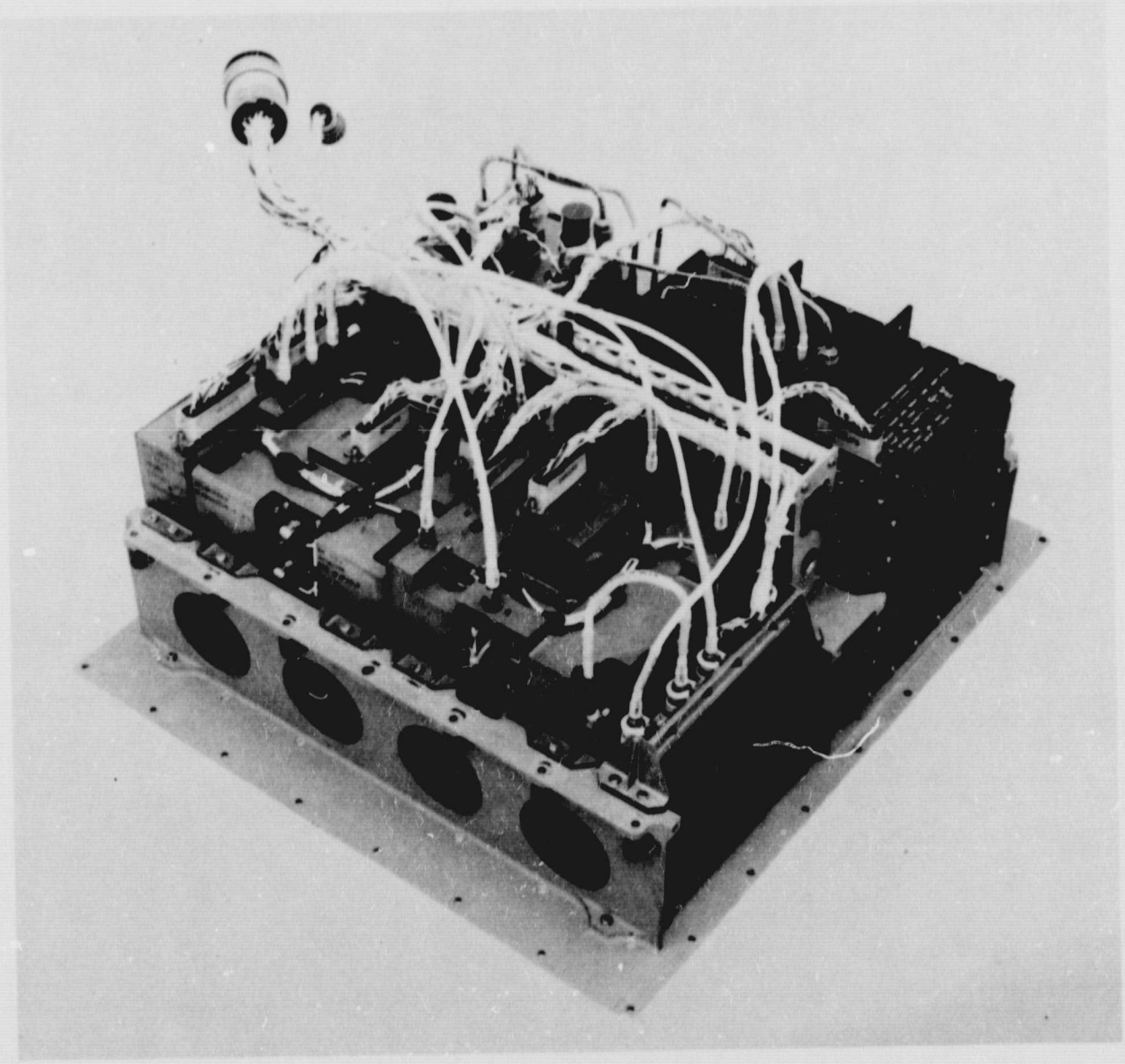

Fig. 1. MM'71 RFS

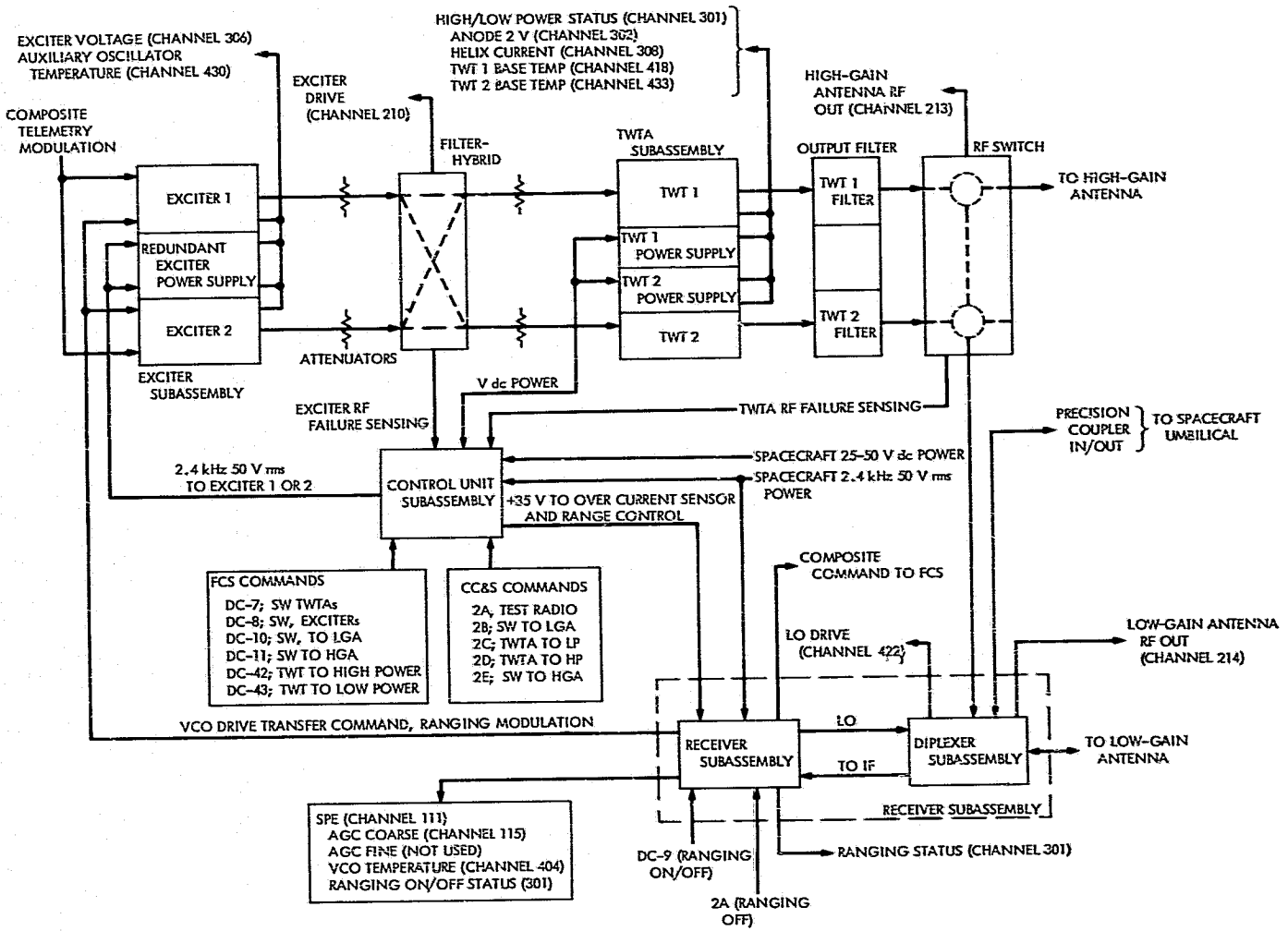

Fig. 2. Radio frequency subsystem block diagram

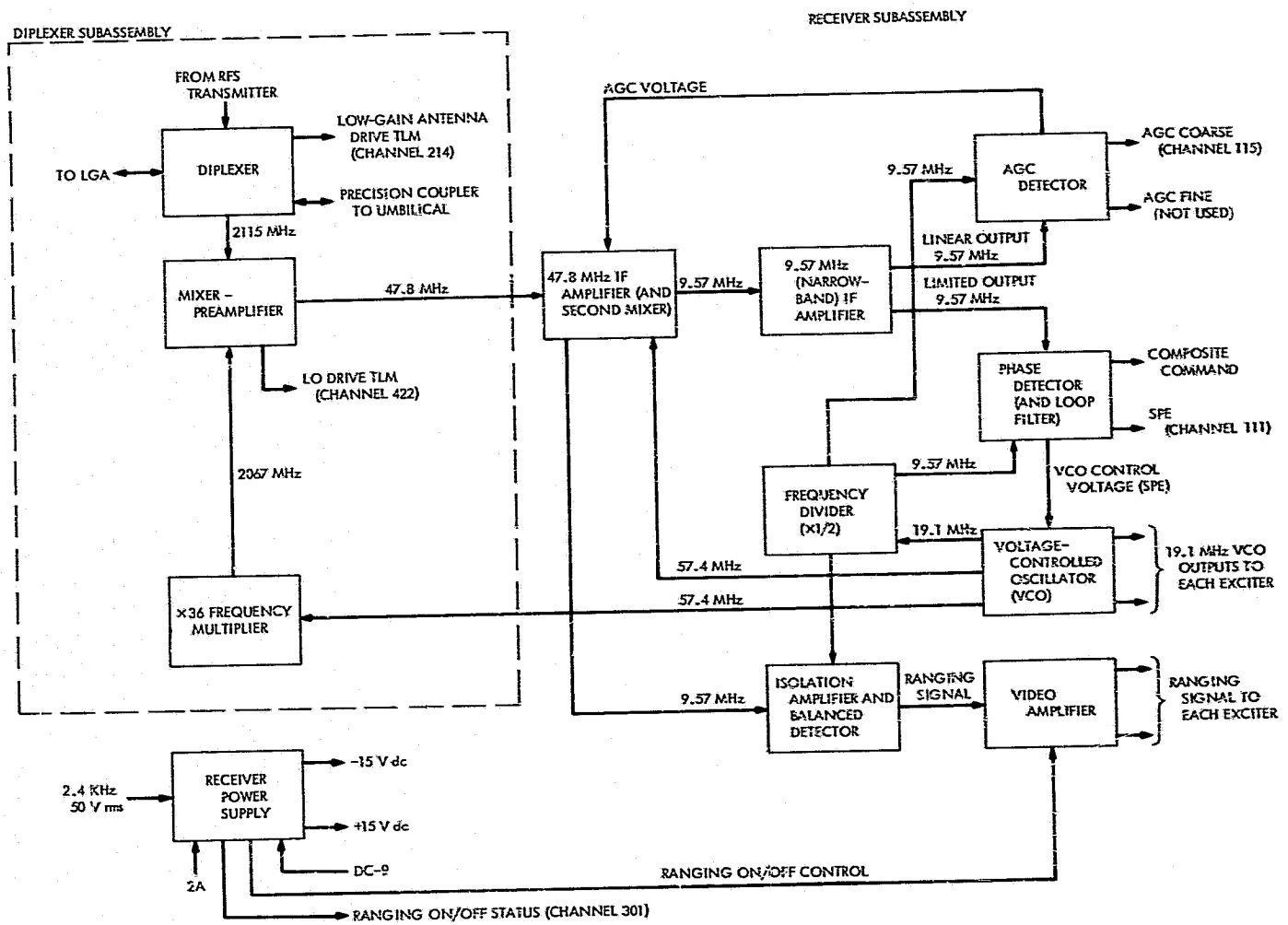

Fig. 3. Receiver block diagram

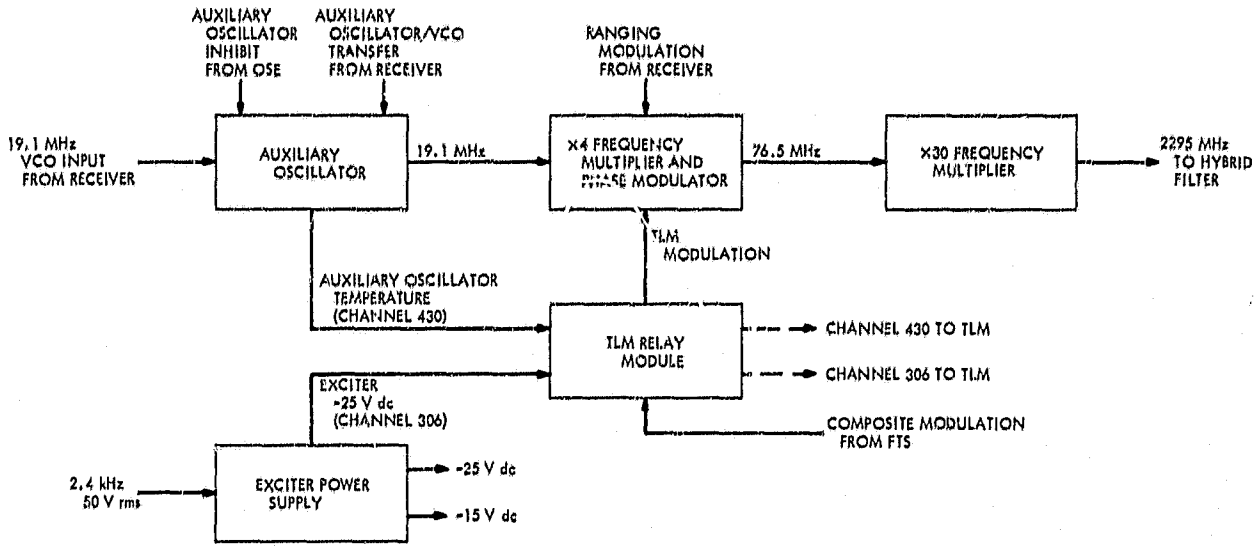

Fig. 4. Exciter block diagram

Fig. 5. ×30 block diagram

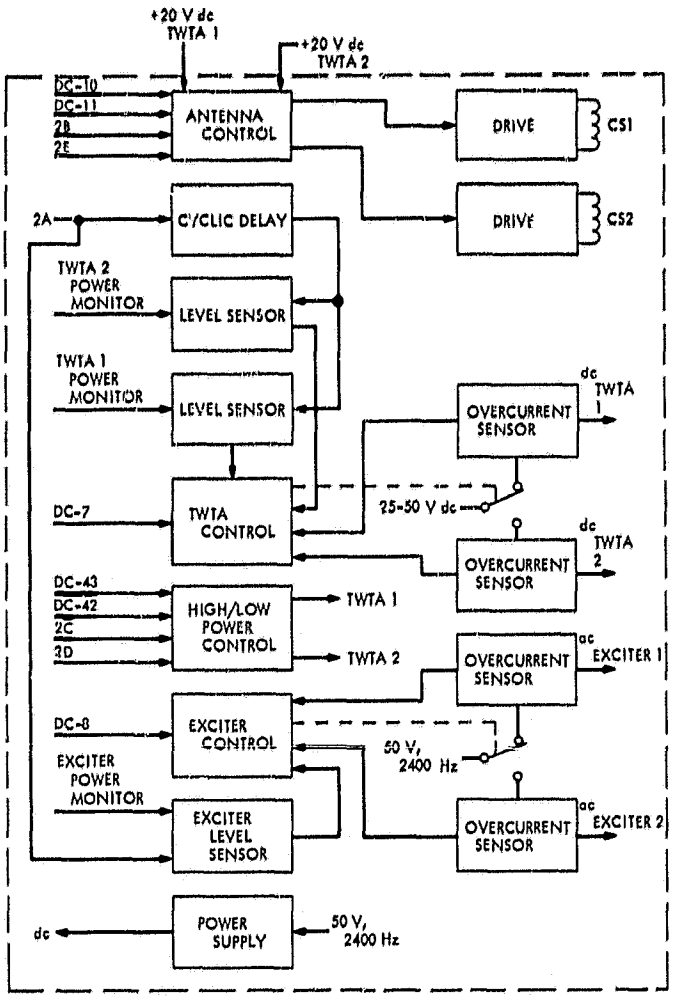

Fig. 6. Control unit block diagram

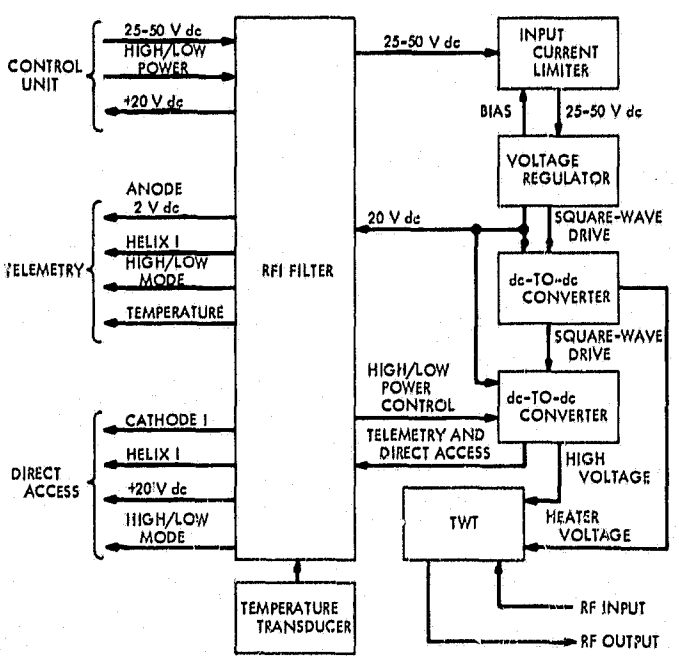

Fig. 7. TWTA block diagram

NASA — JPL — Coml., L.A., Calif.